photonics

MDPI

Article

Diffraction Losses in a Stack of Diamond X-Ray Lenses

Nataliya Klimova * and Anatoly Snigirev

International Science and Research Center "Coherent X-ray Optics for Megascience Facilities", Immanuel Kant Baltic Federal University, 236022 Kaliningrad, Russia
* Correspondence: klimovanb@gmail.com

Abstract: Compound refractive lenses, crafted from single-crystal materials like diamond and silicon, are increasingly favored, particularly in cutting-edge facilities, such as free electron lasers and fourth-generation synchrotrons. These lenses are prized for their low parasitic scattering and resistance to significant radiation doses over extended periods. However, they do encounter a notable drawback known as the "glitch effect", wherein undesired diffraction can occur across various X-ray energies. This phenomenon leads to a decrease in transmitted intensity, impacting experiments, particularly in spectroscopy. Typically, a series of lenses is employed to achieve optimal beam parameters, and each lens has its own spectrum of glitches. This paper presents experimentally measured glitches in stacks of 1, 4, 8, and 16 diamond compound refractive lenses, elucidating the theory behind glitch formation and offering strategies to predict and mitigate glitches in diverse focusing systems employing lenses made from single-crystal materials.

Keywords: X-ray diffraction; compound refractive lenses; single crystal; X-ray optics; cell parameters; crystal orientation

Citation: Klimova, N.; Snigirev, A. Diffraction Losses in a Stack of Diamond X-Ray Lenses. *Photonics* **2024**, *11*, 1097. https://doi.org/10.3390/photonics11121097

Received: 2 October 2024
Revised: 14 November 2024
Accepted: 18 November 2024
Published: 21 November 2024

1. Introduction

Most experiments at modern X-ray facilities, such as synchrotrons and free electron lasers (FELs), require focusing optics either to shape or collimate the beam or increase its intensity at the sample. One of the most commonly used focusing optics for high-energy X-rays in these facilities is compound refractive lenses (CRLs) [1]. CRLs offer several benefits: they can achieve sub-micron spot sizes with high efficiency, cover a broad X-ray energy range (5 to 100 keV), and are easy to integrate into most setups via in-line installation. Due to the fact that the refractive index of most X-ray materials is very close to one, multiple CRLs must be stacked to achieve the desired focal distance. This increases the complexity of the focusing system but also allows it to be tuned for different focal distances and X-ray energies.

Beryllium is the most common material for manufacturing CRLs due to its low absorption coefficient [2,3]. However, beryllium is a toxic material, degrades under high thermal loads, and is polycrystalline, which means CRLs made from it can distort the wavefront of the focused radiation and produce a more parasitic background due to the internal inhomogeneity. Lenses for hard X-rays are often made from aluminum [4], but this material is also polycrystalline and can similarly negatively affect the focused beam.

Alternatively, single-crystal materials, primarily silicon or diamond, can be used to manufacture CRLs [5]. Single crystals offer high quality, thermal stability and reproducibility. Diamond, in particular, is one of the most thermally stable materials [6] and has a relatively low absorption coefficient, especially for hard X-rays. Its robustness and the absence of grain boundaries inside the single crystal make diamond an ideal material for optics [7] at FELs, cavity-based FELs [8], and fourth-generation synchrotrons, where high flux density and outstanding beam quality are essential.

One drawback of X-ray optical elements made from single crystals is diffraction losses, commonly known as "glitches" [9,10]. These occur when, at certain X-ray energies and

crystal orientations, a set of atomic planes in the crystal satisfies the diffraction condition. This causes some incident photons to be diffracted according to Bragg's law, resulting in a drop in the transmitted beam intensity. Glitches are particularly noticeable in spectroscopic experiments, where the energy of the incident X-rays is scanned [11,12]. In such cases, the likelihood of the diffraction condition being satisfied increases with the scanned energy range of X-rays. However, glitches can also occur at fixed energies, making them a general issue for any X-ray experiment involving optics made of single crystals.

The most common X-ray optical element made from single crystals is a monochromator. It consists of one, two, or sometimes more high-quality crystals and is used in experiments requiring a narrow bandwidth of radiation. Some monochromators allow tuning to different energies by rotating the crystals to satisfy Bragg's law for the desired energy or smoothly scanning an energy range by continuously tilting the crystals. The latter approach is commonly used in spectroscopic experiments where a certain energy range needs to be scanned. The broader the scanned energy range, the greater the likelihood of parasitic diffraction satisfying Bragg's law for various atomic planes in the crystal. Consequently, glitches are a well-known issue in X-ray spectroscopy experiments, complicating data analysis [11,13]. Monochromator crystals are typically manufactured to utilize strong reflections, such as 111 or 220 in silicon. As a result, the crystal thickness that X-rays penetrate (known as the extinction length [14]) is relatively small, which limits the extent to which weaker reflections can diffract significant beam energy. The most common method for mitigating these glitches is to measure the beam intensity before and after the sample and then normalize the intensity. This procedure helps minimize the effect of glitches on the resulting spectra; however, as will be shown later, it does not completely resolve monochromator glitch issues—strong monochromator glitches may still appear in the normalized spectrum.

Diffraction losses in CRLs made from single crystals present an even greater challenge: because these devices operate in transmission geometry, the strength of the glitches is proportional to the crystal thickness. In this configuration, even a weak reflection can cause significant beam energy loss if the crystal is thick enough. Another issue with glitches in CRLs is that the focal distance of the focusing system is often quite short, sometimes only a few centimeters. This makes it difficult to place an intensity monitor between the lens and the sample, preventing normalization of the signal after the sample. Therefore, accurately describing and predicting glitches in X-ray optical elements like CRLs is essential.

If the optical element consists of several single crystals (e.g., multiple independent CRLs), the likelihood of glitches increases with the number of crystals in the beam path [15]. It is worth noting that a stack of lenses manufactured from a single-crystal substrate, such as 1D parabolic lenses, behaves as a single crystal, as demonstrated in previous studies [16,17]. CRLs focusing in two directions are typically manufactured individually, and even if several lenses are cut from the same substrate, the final crystallographic orientation of each lens is unique due to small misalignments during assembly. As shown previously, even small rotations of less than 0.1 degrees can cause significant changes in the glitch spectrum [18]. Therefore, each independent lens in a stack must be considered individually.

As mentioned earlier, a stack of lenses made from a single-crystal substrate [19] produces only one set of glitches. Thus, the number of glitches does not depend on the number of lenses in the stack and is much lower than in a stack of N individual single-crystal CRLs. However, the intensity drop associated with each glitch is typically higher for a stack of lenses made from a single-crystal substrate, as it is proportional to the thickness of the crystal with the same orientation. This highlights the main difference between a stack of CRLs made from a single-crystal substrate and a stack of individual CRLs: in the former, fewer glitches are observed, but their intensity is proportional to the thickness of the entire lens stack, whereas, in the latter, the number of glitches increases with the number of CRLs, and the intensity drop for each glitch is proportional to the thickness of the individual lens causing it. Depending on the beamline design and experimental requirements, the focusing system must be chosen: either two 1D stacks of lenses or a single stack of 2D lenses. The

1D lenses are easier and cheaper to manufacture and polish, while 2D lenses are simpler to use. Additionally, because 1D lenses require different focal distances (with orthogonal stacks installed sequentially in the beam), the focused beam exhibits natural astigmatism, which may be undesirable for certain experiments.

Despite the clear advantage of independent lens systems in terms of lower glitch intensity, glitches can still be undesirable in certain experiments, particularly high-precision studies such as high-resolution diffraction and spectroscopy. Furthermore, as already noted, glitches occur more frequently in these systems, increasing the likelihood of negatively impacting the experiment. Therefore, it is essential to accurately describe and predict the occurrence of glitches in systems with multiple lenses.

The main goal of this paper is to demonstrate the ability to characterize and predict glitches in a system made of many individual CRLs, each made of a single-crystal diamond. First, the theory of glitch formation will be introduced, followed by a description of the experiment conducted at the ESRF, with detailed data analysis and results. Practical recommendations will be provided in the conclusions.

2. Materials and Methods

2.1. Theory of Glitches Formation

As previously mentioned, diffraction losses in the intensity of the beam transmitted through an optical element made of a single crystal occur due to parasitic diffraction [16]. This process for a single crystal was described in detail in our previous works [16,17]. Here, we will provide only the most important equations essential for understanding the subsequent sections.

Consider an X-ray beam incident on a crystal with a cubic lattice (with a cell parameter a) along the unit vector $\boldsymbol{e_0}$ (e_{0x}, e_{0y}, e_{0z}). In this case, the energy E_i at which a glitch occurs due to diffraction from a reciprocal lattice point (RLP) with Miller indices h_i, k_i, l_i is given by the following:

$$E_i = -\frac{12398.42\ |\boldsymbol{hkl}|_i^{\,2}}{2\ a\ \boldsymbol{e_0}\cdot\boldsymbol{hkl_i}}, \tag{1}$$

where a is in Å and E_i in eV, and $\boldsymbol{hkl_i}$ is the dimensionless vector formed by the Miller indices and $|\boldsymbol{hkl}| = \sqrt{h^2 + k^2 + l^2}$.

The energy of the X-rays is typically determined by the distance d_{mono} between the atomic planes (characterized by the Miller indices $h_{mono}, k_{mono}, l_{mono}$) of the crystalline monochromator, as well as the angle between these planes and the incident at the monochromator beam ($\theta_i + \Delta\theta$):

$$E_i = \frac{12398.42}{2\ d_{mono}\ \sin(\theta_i + \Delta\theta)} = \frac{12398.42\ |\boldsymbol{hkl}|_{mono}}{2\ a_{mono}\ \sin(\theta_i + \Delta\theta)} \tag{2}$$

where a_{mono} is the monochromator cell parameter, and $\Delta\theta$ is the systematic error in the absolute angle determination.

Considering the Equation (2), the Equation (1) can be rewritten in the following form [17]:

$$e_{0x}h_i + e_{0y}k_i + e_{0z}l_i = -\frac{a_{mono}}{a}\frac{|\boldsymbol{hkl}|_i^{\,2}}{|\boldsymbol{hkl}|_{mono}}\sin(\theta_i + \Delta\theta), \tag{3}$$

Equation (3) can be applied to any glitch with known Miller indices h_i, k_i, l_i and the monochromator angle θ_i corresponding to the measured energy E_i. A systematic error $\Delta\theta$ arises from the uncertainty in the absolute angle of the lattice planes of the monochromator crystal relative to the incident beam; this angle is typically calculated through a calibration procedure using a known absorption edge of a specific material. Consequently, Equation (3) contains four unknowns (the length of unit vector $\boldsymbol{e_0}$ is unity): $e_{0x}, e_{0y}, a, \Delta\theta$. Therefore, at least four energies corresponding to four glitches (with known Miller indices) must be known in order to solve a system of equations like (3) to determine the direction of the

incident beam on the crystal (more precisely, the orientation of the crystal with respect to the beam), its unit cell parameter, and the systematic error in the monochromator angle.

The maximum number of glitches in the absorption spectrum of any single crystal depends on the scanned energy range (from E_1 to E_2) and the volume of the crystal unit cell (which is a^3 for a cubic crystal), as illustrated in Figure 1. In other words, the number of observed glitches corresponds to the number of RLPs located between the two Ewald spheres, with radii proportional to E_1 and E_2 (as shown by the red RLPs in Figure 1):

$$G = C\frac{4}{3}\frac{\pi}{(12398.42)^3}(E_1^3 - E_2^3)a^3, \quad (4)$$

where C is the probability of any reflection being allowed for a given crystal symmetry. For the diamond crystal structure, this coefficient can be easily calculated based on the selection rules, resulting in $C = 0.1875$.

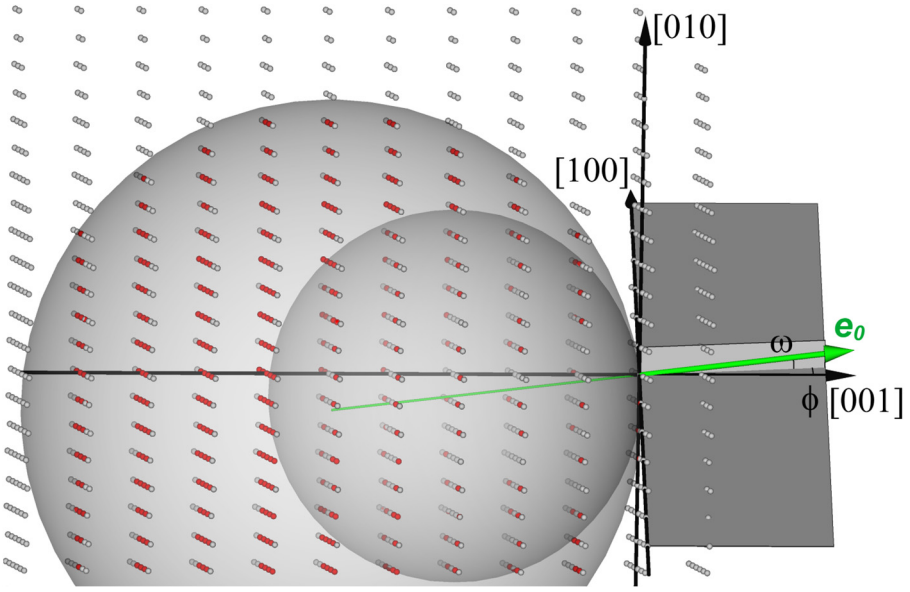

Figure 1. The schematic representation of the reciprocal space of a cubic crystal: the dots representing the RLPs, the smaller and larger Ewald spheres correspond to the beginning (E_1) and end (E_2) of the scanning range. The centers of both spheres lie along the line (green) defined by the direction of the radiation incident on the crystal ($\boldsymbol{e_0}$). This direction forms angles ω and ϕ with respect to the crystalline direction [001]. The red RLPs, located between the two Ewald spheres, are the ones that will be excited during the energy scan and produce glitches in the resulting spectrum.

There may be a small discrepancy between the actual number of reflections calculated using Equation (1) and the number G obtained from Equation (4). This discrepancy arises because Equation (4) represents the volume in reciprocal space between two spheres, while the actual RLPs form a regular grid. Consequently, this difference is merely a quantization error. Another source of discrepancy between the number of glitches observed in the spectrum and the calculated number G may stem from overlapping glitches due to multiple-beam diffraction, particularly when the incident beam is oriented along a crystal zone axis [11,20]. In such cases, the actual number of glitches in the spectrum will be lower. Additionally, some glitches may originate not from the crystal itself but from other sources, such as uncompensated glitches from the monochromator crystals (see example in Section 3). The actual predicted and measured numbers of glitches from the real experiment will be presented in the results section.

If a single lens in the stack is responsible for producing G glitches in the spectrum, a full stack of N_{lenses} will generate a total of $G_{total} = G \times N_{lenses}$. Some glitches in the final spectrum may overlap, so the actual number of glitches to analyze is usually smaller than

G_{total}. The main challenge is that, during measurements, there is no information indicating which lens in the stack produces each glitch observed in the spectrum. Therefore, the first task is to determine the Miller indices of each glitch (indexing) and group the glitches by the lens.

This indexing problem is very similar to the multi-crystal indexing problem in crystallography [21], where a single diffraction pattern contains Bragg peaks originating from multiple crystals. The solution to this problem is typically approached as follows: first, the crystal orientation that explains the majority of observed peaks is identified, and all observed peaks that closely match the predicted ones for that orientation are removed from the list of detected peaks. This process is repeated with the remaining peaks until the orientations and cell parameters of all crystals contributing to the diffraction pattern are determined.

2.2. Experiment

The experiment was performed at the BM31 Swiss-Norwegian Beamlines (SNBL) of the European Synchrotron Radiation Facility (ESRF), France [22]. The radiation generated by a bending magnet passed through the double-crystal Si (111) monochromator and then through the incident intensity monitor (ion chamber I0), through the stack of lenses and through the second ion chamber I1 (Figure 2). Both ionization chambers have a small acceptance aperture, making it nearly impossible for parasitically diffracted radiation to affect the analysis results. All spectra were measured in the range of energies from 10 keV to 20 keV with the energy step of 1 eV. More experimental details can be found in [15,23].

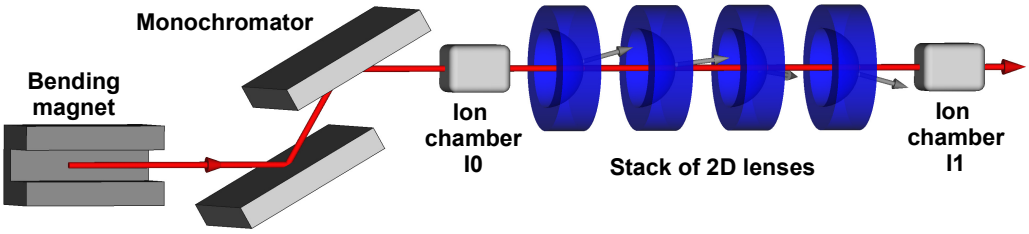

Figure 2. The schematic view of the experiment: the radiation from the bending magnet is monochromatized, and the intensity is measured before the stack of the lenses (I0) and after (I1) by two ion chambers. Gray arrows represent the [001] lattice orientation of each lens; the arrows form angles ω (in the plane) and ϕ (out of plane) with the transmitted beam (red).

To investigate the influence of different numbers of CRLs on the spectrum, four distinct stacks of lenses were prepared, containing 1, 4, 8, and 16 half-lenses made from single-crystal diamonds. All lenses were manufactured by the Technological Institute of Superhard and New Carbon Materials (Russia). Since each stack of lenses contained a different set of CRLs, the results obtained from the smaller stacks could not be used to assist in the indexing of spectra generated by the other stacks.

2.3. Data Processing

The intensity measured after the sample (I1) was normalized by the intensity measured before the sample (I0) to eliminate glitches from the monochromator. Additionally, the resulting I1/I0 spectra were normalized using their smoothed versions to remove absorption effects from the lenses and the electron refills of the storage ring. The exact energies of the glitches in the experimental spectrum were identified using an automated procedure described in our previous work [17] utilizing software developed by us and available on GitHub [24].

The next step is to assign Miller indices to each glitch (indexing glitches) as follows: for various orientations of the beam, incident on the crystal (angles ω and ϕ in Figure 1), and the cell parameter a all possible energies of glitches are calculated using Equation (1). For each measured glitch the nearest simulated glitch energy (corresponding to a set of

Miller indices) is identified, and the average distance between all measured glitches and their nearest simulated counterparts is calculated. The orientation and the cell parameter that result in the smallest average distance are considered a good estimate, allowing each glitch to be assigned the Miller indices. After indexing all experimental glitches, the true orientation, cell parameter, and monochromator angle offset $\Delta\theta$ can be determined using a system of equations of the form (3), requiring at least four correctly indexed glitches. Further details on the indexing of glitches for an individual lens are provided in [16,17].

Indexing glitches caused by multiple lenses is more complex, so to simplify the problem, we determined the monochromator angular offset ($\Delta\theta$ in Equation (2)) separately. This was achieved by using the glitch spectrum measured for a single 2D lens, yielding an offset of $\Delta\theta = 0.01^\circ$. Using a fixed $\Delta\theta$ for all measurements is well justified by the fact that all spectra were measured within a few hours of beamtime without re-adjusting the beamline components—as we observed in our previous studies [16,17] in these conditions the monochromator's angular offset remains constant, and the measured glitch spectra are fully reproducible.

As previously mentioned, indexing glitches from a stack of CRLs assume the diffraction losses are caused by multiple crystals. The number of lenses in the focusing system is known (N_{lenses}), and, as described in the previous section, each lens contributes approximately the same number of glitches to the experimental spectrum. Therefore, the number of fitted glitches for each lens (G_{fit}) corresponds to the total number of glitches found in the spectrum ($G_{observed}$) divided by the number of lenses (N_{lenses}):

$$G_{fit} = \frac{G_{observed}}{N_{lenses}}, \tag{5}$$

The fitting procedure is conducted in three stages: first, the approximate orientation and lattice parameter of each lens are determined using a reduced list of energies (details follow); then, these parameters are refined using the full list of observed glitches; and finally, the orientation of each lens is further refined analytically.

In the first stage, the energy discrepancy between each experimentally observed glitch and the nearest simulated one (based on the current lattice parameter and orientation) is calculated. The list of discrepancies is sorted, and the first G_{fit} discrepancies are averaged. The resulting average discrepancy is used as a metric for the quality of the fit. Once the lattice parameter and orientation for the first lens are determined (with G_{fit} glitches matched), the fitted glitches are removed from the list, and the fitting procedure is repeated for the next lens using the remaining glitches (now with $G_{observed} - G_{fit}$ glitches). This process is repeated until parameters for all N_{lenses} are found.

After determining the parameters for all N_{lenses}, the next step involves refining the parameters within a small angular range (typically $\pm 0.1^\circ$ for each orientation) using the entire list of glitches while assuming only the first G_{fit} glitches should match. This step accounts for the situation where glitches from different lenses overlap in energy, and only one energy is detected in the glitch list.

In the final step, the analytical refinement, as detailed in [16,17], is performed, yielding the true lattice parameter and orientation of each lens.

3. Results

Before presenting the main results, we will show the calculations using Equations (1) and (4) and the measured number of glitches for a single CRL. For a crystal with the cell parameter and orientation described in Table 1, Equation (1) predicts 130 glitches in the energy range from 10,000 to 20,000 eV, while Equation (4) predicts 131 allowed reflections. Automated processing of the measured spectrum detected 108 glitches, some of which were caused by the monochromator, as will be discussed later.

Sections of the measured spectra (11,000 eV to 13,400 eV), along with the simulated glitches for stacks containing one, four, eight, and sixteen lenses, are presented in Figure 3.

The corresponding cell parameters and orientations for each lens in the different stacks are summarized in Tables 1–3.

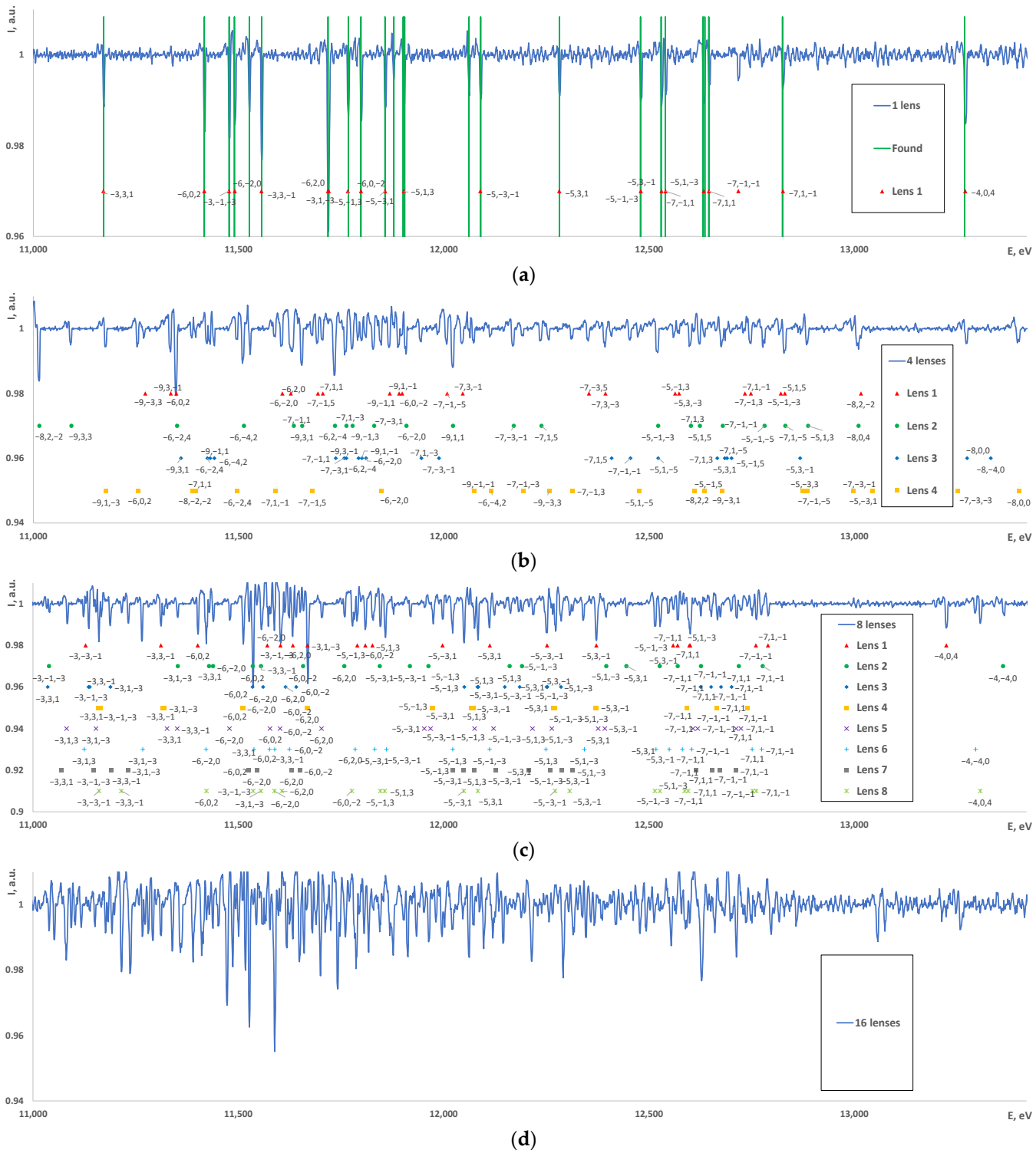

Figure 3. Portions of the normalized measured spectra (blue curves) for stacks containing (**a**) one, (**b**) four, (**c**) eight, and (**d**) sixteen individual 2D half-lenses made from single-crystal diamond. The predicted glitches for each lens are shown as dots with the corresponding Miller indexes. In the first plot, the identified glitches are indicated by vertical green lines.

Table 1. Orientations and the unit cell parameters for the lenses in a stack containing a single lens.

Lens	UC, Å	ω, °	ϕ, °	Error, eV
Lens 1	3.56744	2.8222	1.6937	0.670

Table 2. Orientations and the unit cell parameter for the lenses in a stack containing four lenses.

Lens	UC, Å	ω, °	ϕ, °	Error, eV
Lens 1	3.5673	4.0647	0.1547	0.611
Lens 2	3.5672	4.1205	1.6424	0.424
Lens 3	3.5673	2.8556	2.5933	0.935
Lens 4	3.5674	2.5596	6.3033	0.828

Table 3. Orientations and the unit cell parameter for the lenses in a stack containing eight lenses.

Lens	UC, Å	ω, °	ϕ, °	Error, eV
Lens 1	3.5673	3.0214	0.4544	0.451
Lens 2	3.5673	0.9041	2.3676	0.644
Lens 3	3.5671	0.7885	0.4039	0.543
Lens 4	3.5675	1.1816	1.1554	0.453
Lens 5	3.5673	0.1805	1.6621	0.788
Lens 6	3.5673	0.3597	2.6872	0.378
Lens 7	3.5672	0.9317	0.6331	0.725
Lens 8	3.5671	2.6294	0.1505	0.619

In order to avoid overloading the plots with extra information, the automatically detected glitches [17] are presented only in Figure 3a. As seen in Figure 3a, some glitches were too weak to be detected (such as the one at 12,717 eV, with indices −7, −1, 3). At the same time, some glitches were detected but not indexed, such as at 11,526 eV, 11,878 eV, and 12,062 eV. These three glitches originated from the monochromator and were not fully eliminated during the I1/I0 normalization process. The intensity of these uncorrected monochromator glitches is comparable to that of actual lens glitches, illustrating that simple normalization I1/I0 is insufficient—a more sophisticated method is required to address monochromator glitches, but this will be covered in a separate study in future publications.

Undetected real glitches, along with the monochromator and noise glitches detected by the automated search procedure, complicate the interpretation of the measured spectra. With more lenses in the stack, fewer glitches per lens are detected. As seen in Figure 3, with an increasing number of lenses contributing to the spectrum, the intensity drops become less distinct and appear more like noise. Despite these challenges, the automatic procedure developed was able to accurately predict the glitches for stacks of one, four, and eight lenses.

The best validation of the accuracy of the determined parameters is the absence of simulated glitches in regions where no clear experimental glitches were observed. These regions are at the positions of the legends of Figure 3a–c: 12,850–13,250 eV for a single lens, 13,050–13,230 eV for four lenses and 12,800–13,200 eV for eight lenses. The entire data processing procedure relied solely on the detected glitches without imposing any constraints on unobserved glitches. The absence of both measured and simulated glitches in the same energy ranges provides independent confirmation of the successful determination of the lenses' parameters.

From Tables 2 and 3, it can be seen that some lenses in the four- and eight-lens stacks show higher fitting errors for the glitches compared with the single lens (Table 1). This is likely because some glitches may have been incorrectly attributed to a lens, thereby increasing the average error. Additionally, non-compensated monochromator glitches may be assigned to a specific lens, further increasing the error.

It has to be mentioned that there is no reliable way to determine the physical order of the lenses in the stack and how it corresponds to the order of the lenses in Tables 2 and 3.

The "strength" of each glitch depends primarily on the thickness of the material through which the X-rays pass and is mostly unaffected by the lens's position in the stack. Therefore, the labeling in the plots and tables (e.g., lens 1, lens 2, etc.) is arbitrary and reflects only the order in which the parameters of the lenses were determined by the algorithm.

4. Discussion

The proposed procedure for processing the glitch spectrum from multiple independent crystals did not work effectively in the case of the spectrum obtained from a stack of sixteen two-dimensional lenses (Figure 3d). Several factors contributed to the failure of the method in this scenario:

- In the experimental spectrum of the 16-lens stack, 229 glitches were detected using an automatic peak search procedure (including some uncorrected monochromator glitches). However, each lens in the energy range of 10 to 20 keV can generate around 130 glitches, meaning that the entire stack could produce about 2100 glitches. The relatively high noise level, which was comparable to the intensity of most detected glitches, led to the identification of far fewer glitches than expected. This noise increased the likelihood of misidentifying which of the 229 experimental glitches corresponded to the 2100 theoretically possible glitches.
- The measurements were taken with a 1 eV energy step, resulting in approximately 10,000 data points in the spectrum. Given the total number of potential glitches (2100) and their average full-width-at-half-maximum (FWHM) of 2–5 eV, the probability of glitches overlapping was very high. When multiple glitches from different lenses overlap, their individual energies cannot be determined with sufficient accuracy. What facilitated our analysis of the eight-lens stack is the fact that glitches are not uniformly distributed across the energy range; thus, some isolated glitches can still be identified even in systems with more than ten lenses.
- The accuracy of determining the experimentally measured glitch energy was limited by the energy step size (1 eV), introducing further errors that affected subsequent data processing steps. This energy step was justified for the Si 111 monochromator used in the experiment. Si 311 monochromator, available at BM31 and many other beamlines, allows measurements with better energy resolution.

Considering these challenges, the measurement and data processing procedures must be improved for large numbers of simultaneously illuminated independent monocrystalline lenses. Future improvements to the procedure for stacks containing many lenses may include measuring the spectrum with smaller energy steps and obtaining better statistics at each energy point either by increasing the measurement time at each point or by optimizing the ion chamber parameters. This would enable more precise and reliable glitch detection in the experimental spectrum. Additionally, the glitch detection procedure could be enhanced by fitting each detected glitch with a Gaussian curve, allowing for a more accurate determination of glitch energies. This method would also help exclude glitches whose FWHM does not match most others. For very broad glitches, fitting multiple Gaussian curves could be used to distinguish overlapping glitches.

We believe that the most efficient way to improve the fitting procedure is to incorporate not only the energy information of the glitches but also their intensity. For instance, the most intense glitches could be fitted first using only the strongest reflections, and the crystal orientations could be refined with all identified glitches afterward. The intensity of the glitches serves as a significant additional constraint, and we believe it can aid in extending the proposed method to more complex focusing systems. We plan to extend the data processing pipeline to consider the intensity of the glitches in future studies.

In focusing systems where lenses can be removed and reinserted with reproducible orientation and positioning (such as in modern transfocators [25]), the lenses could be characterized in smaller groups. In this case, glitch spectra could be measured for groups of 4–8 lenses, allowing for at least an approximate determination of each lens's orientation. In our previous studies [16,17], we already demonstrated that the glitch spectrum is com-

pletely reproducible as long as the orientation of the beam with respect to the lens remains unchanged. By utilizing the determined approximate orientation of each lens, the energy scan can be repeated for the entire stack of lenses required for a given experiment. With this prior information for each lens, a small energy scan (typically around 1 keV) will be sufficient to predict the glitches of the whole stack of CRLs for any energy.

The glitch spectrum for each lens depends primarily on the orientation of its crystal lattice relative to the beam. This means that surface orientation, including the so-called miscut, and the lens's mounting method have a significant impact. Due to the high sensitivity of glitches to crystal orientation, it is highly unlikely that two lenses will produce similar glitch spectra. This fact can be exploited to conduct measurements without glitches in specific energy ranges or to avoid intensity instabilities caused by glitches at fixed energy. These measurements could be carried out as follows: first, the glitch spectrum for each lens is determined (to optimize beamtime efficiency, this can be performed for several lenses simultaneously using the procedure described in this paper). Then, only the lenses that do not produce strong glitches in the desired energy range are used for focusing. This strategy can be used for focusing systems, where the lenses can be removed or inserted in a reproducible way, like transfocators. Although this strategy may limit focusing options, it will completely eliminate the influence of glitches on the measurements.

As mentioned in the introduction, the focusing system may be constructed using either 1D or 2D CRLs. In the 1D case, two orthogonal stacks of lenses are typically used, with each stack comprising a single crystal from which individual CRLs are cut. In contrast, in the 2D design, each CRL in the stack is individually made and mounted, so the stack represents multiple individual crystals. Consequently, for 1D lenses, the thickness of a single crystal that X-rays penetrate can be relatively large, leading to diffraction losses that may reach 80% of the beam intensity or even higher [15]. For a stack of 2D lenses, however, the typical intensity loss is only a few percent (see Figure 3). This difference in glitch intensity between the two CRL designs can inform the planning of new beamlines. If the beamline operates at a single wavelength, two 1D stacks, pre-tested for the absence of glitches near the desired energy, can be used (considering only diffraction losses). This approach is also suitable for spectroscopic applications where certain small energy regions can be disregarded during data analysis. However, if energy scans are planned on future beamlines and no energy range can be omitted, 2D lenses are a better option, particularly if the focal distance is relatively large and an incident intensity monitor can be positioned after the lenses.

5. Conclusions

Modern synchrotrons and free-electron lasers require high-quality X-ray optics. Single crystals of silicon and diamond are the best materials for manufacturing such optics, which are becoming increasingly popular due to the demand for high-quality lenses at fourth-generation synchrotrons. However, one major disadvantage of X-ray optics made from single crystals is the potential diffraction losses in beam intensity due to parasitic diffraction. The likelihood of encountering glitches increases with the number of single crystals in the optical system.

Each lens in a stack is typically quite thin, so the intensity drop caused by a glitch in a single lens usually reaches 2–3% [15]—a stark contrast to stacks of lenses cut from a single substrate, where intensity loss can reach 80% or higher [15,17]. While the small intensity drop in the independent compound refractive lens may be negligible for some experiments, it can be critical in studies where the expected effect is small, as these sharp intensity changes can significantly affect results.

The main challenge in analyzing glitches in systems with multiple independent single crystals lies in the fact that the measured spectrum contains glitches from all optical elements combined into a single plot. Therefore, in addition to assigning Miller indices to each glitch, the glitches must be grouped by lens. This makes characterizing glitches caused by a stack of lenses far more complex than for a single lens.

In this paper, we developed a method for processing the glitch spectrum generated by several independent crystals and demonstrated the successful determination of the cell parameters and orientation of each lens in a stack containing up to eight two-dimensional half-lenses made of single-crystal diamonds based on a single glitch spectrum measured for the entire stack. However, for stacks containing more lenses (16 in this case), both the measurement and data processing procedures require improvement.

Although the glitches from the 16-lens stack could not be successfully processed at this stage, we are confident that with improvements in measurement strategy and more advanced data processing techniques, glitches from up to 20 lenses could still be successfully analyzed. For even larger stacks, the number of glitches in the spectrum would become overwhelming, necessitating a different approach: the stack would need to be divided into smaller sub-stacks, and each would be processed individually to determine approximate cell parameters and orientation for each lens. The spectrum of the entire system could then be analyzed by refining these initial approximations for each lens.

The methods proposed in this paper for handling diffraction losses from multiple single crystals can be applied not only to CRL stacks but also to other optical elements. For example, in certain applications, high-quality attenuators that do not introduce additional irregularities in the wavefront, especially at fourth-generation synchrotrons, are needed. A stack of variable attenuators could be made from silicon slabs, which are inserted into the beam to achieve the desired attenuation factor. Such a system would also produce glitches at specific energies, and these glitches could be characterized and predicted using the method described in this paper.

Author Contributions: Conceptualization, A.S.; methodology, N.K.; validation, N.K.; formal analysis, N.K.; investigation, N.K. and A.S.; resources, A.S.; data curation, N.K.; writing—original draft preparation, N.K.; writing—review and editing, N.K.; visualization, N.K.; supervision, A.S.; project administration, A.S.; funding acquisition, A.S. All authors have read and agreed to the published version of the manuscript.

Funding: This research received no external funding.

Institutional Review Board Statement: Not applicable.

Informed Consent Statement: Not applicable.

Data Availability Statement: All raw data, as well as the developed programs used in this study, are available for download at GitHub [24].

Acknowledgments: We would like to express our gratitude to Oleksandr Yefanov (CFEL@DESY, Germany) for his innovative ideas, for writing the programs, for helping with data processing, and for his contributions to the manuscript. Unfortunately, due to the current DESY restrictions, O.Y. cannot be listed as a co-author of this paper. We also extend our thanks to the experimental team for their support in conducting the experiment at ESRF in 2016.

Conflicts of Interest: The authors declare no conflicts of interest.

References

1. Snigirev, A.; Kohn, V.; Snigireva, I.; Lengeler, B. A Compound Refractive Lens for Focusing High-Energy X-Rays. *Nature* **1996**, *384*, 49–51. [CrossRef]
2. Beguiristain, H.R.; Cremer, J.T.; Piestrup, M.A.; Gary, C.K.; Pantell, R.H. X-Ray Focusing with Compound Lenses Made from Beryllium. *Opt. Lett.* **2002**, *27*, 778. [CrossRef]
3. Schroer, C.G.; Kuhlmann, M.; Lengeler, B.; Gunzler, T.F.; Kurapova, O.; Benner, B.; Rau, C.; Simionovici, A.S.; Snigirev, A.A.; Snigireva, I. Beryllium Parabolic Refractive X-Ray Lenses. In *Design and Microfabrication of Novel X-Ray Optics*; Mancini, D.C., Ed.; SPIE: Seattle, WA, USA, 2002; p. 10.
4. Lengeler, B.; Schroer, C.G.; Richwin, M.; Tümmler, J.; Drakopoulos, M.; Snigirev, A.; Snigireva, I. A Microscope for Hard x Rays Based on Parabolic Compound Refractive Lenses. *Appl. Phys. Lett.* **1999**, *74*, 3924–3926. [CrossRef]
5. Nöhammer, B.; Hoszowska, J.; Freund, A.K.; David, C. Diamond Planar Refractive Lenses for Third- and Fourth-Generation X-ray Sources. *J. Synchrotron Radiat.* **2003**, *10*, 168–171. [CrossRef] [PubMed]

6. Antipov, S.; Baryshev, S.; Baturin, S.; Chen, G.; Kostin, R.; Stoupin, S. Thermal Analysis of the Diamond Compound Refractive Lens. In *Advances in X-Ray/EUV Optics and Components XI*; Khounsary, A.M., Goto, S., Morawe, C., Eds.; SPIE: San Diego, CA, USA, 2016; p. 99630R.
7. Antipov, S.; Baryshev, S.V.; Butler, J.E.; Antipova, O.; Liu, Z.; Stoupin, S. Single-Crystal Diamond Refractive Lens for Focusing X-Rays in Two Dimensions. *J. Synchrotron Radiat.* **2016**, *23*, 163–168. [CrossRef] [PubMed]
8. Liu, P.; Pradhan, P.; Shi, X.; Shu, D.; Kauchha, K.; Qiao, Z.; Tamasaku, K.; Osaka, T.; Zhu, D.; Sato, T.; et al. X-Ray Optics for the Cavity-Based X-Ray Free-Electron Laser. *J. Synchrotron Radiat.* **2024**, *31*, 751–762. [CrossRef] [PubMed]
9. Bauchspiess, K.R.; Crozier, E.D. Crystal Glitches of X-ray Monochromators. In *EXAFS and Near Edge Structure III, Proceedings of an International Conference, Stanford, CA, USA, 16–20 July 1984*; Springer: Berlin/Heidelberg, Germany, 1984; pp. 514–516, ISBN 978-3-642-46524-6.
10. van Zuylen, P.; van der Hoek, M.J. Some Considerations on Glitches and the Design of a Double Crystal Monochromator with Bent Crystals. In *Soft X-Ray Optics and Technology*; Koch, E., Schmahl, G.A., Eds.; SPIE: Berlin, Germany, 1986; pp. 248–252.
11. Dobson, B.R.; Hasnain, S.S.; Morrell, C.; Konigsberger, D.C.; Pandya, K.; Kampers, F.; van Zuylen, P.; van der Hoek, M.J. Non-normalization Behavior of Crystal Glitches in an EXAFS Spectrum: Is It Possible to Remove Crystal Glitches? *Rev. Sci. Instrum.* **1989**, *60*, 2511–2514. [CrossRef]
12. Bridges, F.; Li, G.G.; Wang, X. Monochromator-Induced Glitches in EXAFS Data I. Test of the Model for Linearly Tapered Samples. In *Nuclear Instruments and Methods in Physics Research Section A: Accelerators, Spectrometers, Detectors and Associated Equipment*; Elsevier: Amsterdam, The Netherlands, 1992; Volume 320, pp. 548–555. [CrossRef]
13. Hodgson, K.O.; Hedman, B.; Penner-Hahn, J.E. Softcover reprint of the original. In *EXAFS and Near Edge Structure III, Proceedings of an International Conference, Stanford, CA, USA, 16–20 July 1984*, 1st ed.; Springer: Berlin/Heidelberg, Germany, 1984; ISBN 978-3-642-46524-6.
14. Authier, A.; Lagomarsino, S.; Tanner, B.K. (Eds.) *X-Ray and Neutron Dynamical Diffraction: Theory and Applications*; NATO ASI Series; Springer US: Boston, MA, USA, 1996; Volume 357, ISBN 978-1-4613-7696-5.
15. Polikarpov, M.; Emerich, H.; Klimova, N.; Snigireva, I.; Savin, V.; Snigirev, A. Spectral X-Ray Glitches in Monocrystalline Diamond Refractive Lenses. *Phys. Status Solidi B* **2018**, *255*, 1700229. [CrossRef]
16. Klimova, N.; Yefanov, O.; Snigireva, I.; Snigirev, A. Determination of the Exact Orientation of Single-Crystal X-Ray Optics from Its Glitch Spectrum and Modeling of Glitches for an Arbitrary Configuration. *Crystals* **2021**, *11*, 504. [CrossRef]
17. Klimova, N.; Snigireva, I.; Snigirev, A.; Yefanov, O. Using Diffraction Losses of X-Rays in a Single Crystal for Determination of Its Lattice Parameters as Well as for Monochromator Calibration. *J. Synchrotron Radiat.* **2022**, *29*, 369–376. [CrossRef] [PubMed]
18. Klimova, N.; Snigireva, I.; Snigirev, A.; Yefanov, O. Suppressing Diffraction-Related Intensity Losses in Transmissive Single-Crystal X-Ray Optics. *Crystals* **2021**, *11*, 1561. [CrossRef]
19. Schroer, C.G.; Kuhlmann, M.; Hunger, U.T.; Günzler, T.F.; Kurapova, O.; Feste, S.; Frehse, F.; Lengeler, B.; Drakopoulos, M.; Somogyi, A.; et al. Nanofocusing Parabolic Refractive X-Ray Lenses. *Appl. Phys. Lett.* **2003**, *82*, 1485–1487. [CrossRef]
20. Tang, Z.; Zheng, L.; Chu, S.; Wu, M.; An, P.; Zhang, L.; Hu, T. Optimal Azimuthal Orientation for Si(111) Double-Crystal Monochromators to Achieve the Least Amount of Glitches in the Hard X-Ray Region. *J. Synchrotron Radiat.* **2015**, *22*, 1147–1150. [CrossRef] [PubMed]
21. White, T.A.; Kirian, R.A.; Martin, A.V.; Aquila, A.; Nass, K.; Barty, A.; Chapman, H.N. *CrystFEL*: A Software Suite for Snapshot Serial Crystallography. *J. Appl. Crystallogr.* **2012**, *45*, 335–341. [CrossRef]
22. BM31 Swiss Norwegian Beamlines. Available online: https://www.esrf.fr/UsersAndScience/Experiments/CRG/BM01/bm01b (accessed on 10 November 2024).
23. Zhang, Q.; Polikarpov, M.; Klimova, N.; Larsen, H.B.; Mathiesen, R.; Emerich, H.; Thorkildsen, G.; Snigireva, I.; Snigirev, A. Investigation of 'glitches' in the Energy Spectrum Induced by Single-Crystal Diamond Compound X-Ray Refractive Lenses. *J. Synchrotron Radiat.* **2019**, *26*, 109–118. [CrossRef] [PubMed]
24. Yefanov, O. Glitches Simulation and Processing. Available online: https://github.com/XrayViz/Glitches (accessed on 20 October 2024).
25. Vaughan, G.B.M.; Wright, J.P.; Bytchkov, A.; Rossat, M.; Gleyzolle, H.; Snigireva, I.; Snigirev, A. X-Ray Transfocators: Focusing Devices Based on Compound Refractive Lenses. *J. Synchrotron Radiat.* **2011**, *18*, 125–133. [CrossRef] [PubMed]